

Measurement of cation diffusion in magnesium oxide by determining the Mg ^{18}O buildup produced by an electric field

J. R. Martinelli

Department of Materials Science and Engineering, Vanderbilt University, Nashville, Tennessee 37235

E. Sonder

Solid State Division, Oak Ridge National Laboratory, Oak Ridge, Tennessee 37831

R. A. Weeks

Department of Materials Science and Engineering, Vanderbilt University, Nashville, Tennessee 37235

R. A. Zuhr

Solid State Division, Oak Ridge National Laboratory, Oak Ridge, Tennessee 37831

(Received 31 January 1985)

Magnesium self-diffusion in MgO crystals has been studied over the temperature range 1100–1250 K with the use of the nuclear reaction $^{18}\text{O}(p,\alpha)^{15}\text{N}$. Magnesium drift due to an electric field was determined, and from the buildup of Mg ^{18}O at the cathode, diffusion coefficients and the activation energy for magnesium diffusion were determined. Values for magnesium self-diffusion coefficients are consistent with extrapolation of the values obtained at higher temperatures. The transference numbers obtained are within the range of those measured previously.

I. INTRODUCTION

Mass transport in insulating oxides is driven by concentration gradients, temperature gradients, stress fields, and electric fields. Many physical properties are affected by this transport. The effects of electric fields, for example, may be enhancing mass transport shorten the useful life of electrically insulating oxides in high-temperature environments. Advanced systems for energy conversion, such as magnetohydrodynamic generators, require insulating materials capable of withstanding corrosive environments at high temperatures. MgO has been considered a potential material for this application. However, its electrical properties degrade¹ owing to mass transport² under the influence of electric fields of magnitude on the order of 10^3 V/cm at $T \geq 1000^\circ\text{C}$. Partly for this reason, and because MgO is a relatively simple "model" oxide, mass transport under the influence of electric fields is investigated in MgO.

The study of electric-field effects on ionic diffusion has provided valuable information about the charge state of diffusing defects. The presence of electric fields produces a shift of the tracer-concentration profile if the defect in question is charged; the mobility of the diffusing species can be estimated from this shift. The effects of electric fields on the diffusion of atomic species have been used in the past to identify the contribution of charged vacancies to the diffusion process in alkali halides.^{3,4} There have also been some studies of the effects of electric fields on solid-state reactions in oxide systems.⁵⁻⁷

In compounds such as MgO, diffusion occurs both in the cation and anion sublattices. There may be ambiguity as to which sublattice is involved in producing particular

experimental results. For example, measurements aimed at determining electric-field-induced oxygen-ion drift may yield results on cation diffusion, as is demonstrated in this paper. In experiments in which ^{18}O exchange between an oxide compound and the ambient gas is measured, electric fields produce two effects: (1) They give rise to a unidirectional drift of oxygen ions that is superposed on the normal diffusion broadening of the concentration profile, and (2) they produce a similar effect in the cation sublattice. Upon arriving at the sample surface, the drifting cations react with the ambient $^{18}\text{O}_2$, creating a metal-oxide layer. In MgO the magnesium mobility is about two orders of magnitude greater than that of oxygen;⁸ thus the second mechanism, if present, should produce effects that exceed those due to oxygen diffusion. Hence these effects should be easily measured.

In the present work evidence is presented of Mg-ion drift to the cathode of MgO single crystals subjected to electric fields. Cation-vacancy-diffusion coefficients, transference numbers, and magnesium-diffusion coefficients are estimated from the thickness of a Mg ^{18}O layer formed at the cathode interface.

II. EXPERIMENTAL

The method employed in this work makes use of the nuclear reaction $^{18}\text{O}(p,\alpha)^{15}\text{N}$. This reaction exhibits a large resonance at 629 keV; the reaction yield in the vicinity of this resonance is used to measure the amount of ^{18}O that reacts at the cathode surface when an MgO crystal is subjected to an electric field while exposed to an $^{18}\text{O}_2$ -enriched atmosphere. α -particle yields produced by the reaction are measured as a function of incident proton en-

TABLE I. Impurities in MgO in units of mol ppm.

	Sample nominally pure	Sample doped
Al	65	
V	16	
Cr	6	1154
Mn	1	
Fe	51	
Na	226	

ergy. The total α -particle count is then plotted against the proton energy, resulting in a plot that we call the "excitation curve." When the initial proton energy is equal to 629 keV, the resonant reaction occurs for ^{18}O at the surface of the material; for energies slightly greater than 629 keV, the reaction will be induced at a depth at which the energy has decreased to 629 keV. Thus the method yields not only the total amount of ^{18}O but also information on the depth distribution.

MgO crystals were purchased from Tateho Chemical Industries.⁹ Table I shows the impurities detected by neutron activation analysis in the samples used for the present study. These samples were cut in slabs $1 \times 0.6 \times 0.1 \text{ cm}^3$ or $1 \times 1 \times 0.1 \text{ cm}^3$ with faces parallel to the crystallographic (100) planes. After having been ground with a series of successively finer abrasives, each sample was further mechanically polished with $0.3\text{-}\mu\text{m}$ alumina and chemically polished with a solution of 85% H_3PO_4 at 150°C . Preanneals at 1400°C for 4 h in air were performed after these treatments to reduce the dislocation density.¹⁰

The diffusion anneals were performed over the range of temperature $800\text{--}1000^\circ\text{C}$ in a $95\%\text{-}^{18}\text{O}_2$ -enriched atmosphere with applied electric fields ranging from $0\text{--}3000 \text{ V/cm}$, during intervals of $24\text{--}96 \text{ h}$. Figure 1 shows the experimental apparatus. Samples were inserted in a

quartz tube and compressed between two platinum-gauze electrodes by means of springs that remained outside the hot zone of the furnace. To keep the pressure uniformly distributed over the sample, two perforated discs made of alumina were used to press the electrodes against the samples. The samples, in their holders, were inserted in the furnace after the latter reached a stable temperature. The system was then evacuated to $1.3 \times 10^{-3} \text{ Pa}$ (10^{-5} Torr) and filled with 1 atm of $95\% \text{ }^{18}\text{O}_2$, $5\% \text{ }^{16}\text{O}_2$. During the process of filling, the gas passed through a cold trap in order to remove any residual water. The cold trap was cooled to $\sim 175 \text{ K}$ with methanol slush. Samples of gas were collected before and after the anneals and analyzed by mass spectrometry in order to monitor the variation of the isotopic concentration.

The electric field was applied by an external power supply and the current was measured by a digital electrometer in series with the sample, the power supply, and a resistance of 100Ω . Electrical connections to one of the electrodes was made with a Pt:Pt 10% Rh thermocouple which was also used to monitor the temperature of the sample. At the end of each anneal, the samples were cooled inside the furnace to room temperature at an initial cooling rate of $\sim 10^\circ\text{C}/\text{min}$. Before withdrawing the samples, the remaining gas was stored in a sorption pump containing zeolite. The quartz tube was then filled with dry air and the sample withdrawn.

The arrangement for the magnesium oxide sample containing 1154 mol ppm chromium was slightly different. A sandwich was made of it and a nominally pure MgO sample; the anode was placed between the two samples, and the cathode of each sample was brought out of the furnace separately. Thus both samples experienced identical treatment.

After annealing, the sample surfaces were covered with 20 nm of aluminum by sputtering an aluminum target with argon. Nuclear microanalysis was performed, as

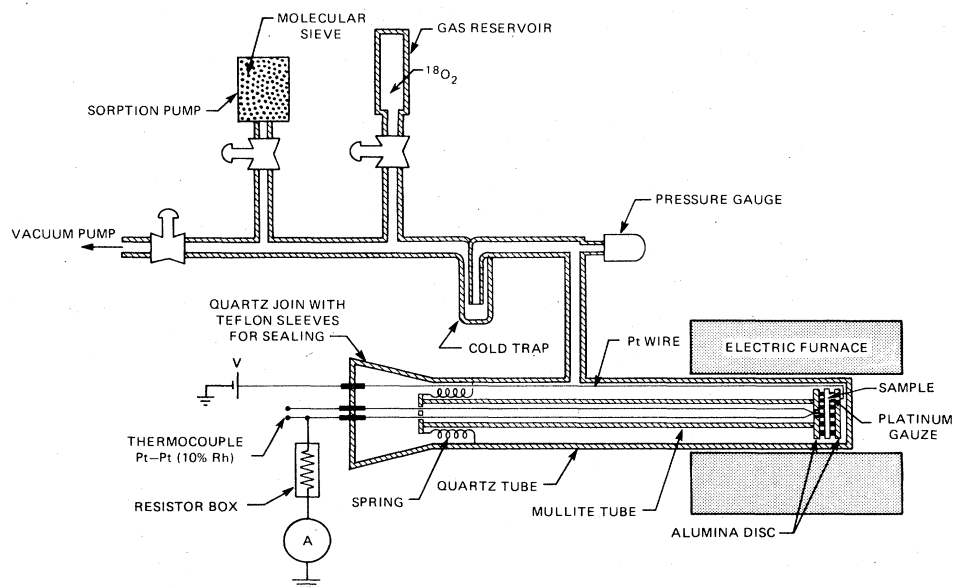


FIG. 1. Schematic diagram of the gas-solid isotope exchange apparatus.

mentioned above, by inducing the nuclear reaction $^{18}\text{O}(p,\alpha)^{15}\text{N}$. The proton beam was produced by a Van de Graaff accelerator; by varying the proton beam energy from 629 to 700 keV the reaction was induced for depth from 0 to 800 nm in the MgO samples. The total α -particle count was recorded for each incident proton energy to produce an excitation curve. The samples were oriented 7° off the $\langle 100 \rangle$ direction to avoid channeling.

The α particles were detected with a silicon surface barrier detector (ORTEC model No. TE-13-100-100) located 90 mm from the center of the goniometer and making an angle of 150° with respect to the incident proton beam direction. A thin aluminized Mylar film $12.7\ \mu\text{m}$ thick covered the detector to shield it from backscattered protons. The beam current ranged from 50 to 150 nA and the integrated current for each run was $20\ \mu\text{C}$.

A disc of zirconium with a 15-nm film of Zr^{18}O_2 on the surface was used as a standard in order to provide an energy calibration and to compensate for accelerator-parameter changes that may have occurred when the accelerator was used for other experiments.

III. DATA ANALYSIS

Although the ^{18}O concentration profile cannot be extracted directly from the excitation curves without a deconvolution, the results can be analyzed quantitatively by generating excitation curves from the convolution of assumed concentration profiles, and by comparing the resulting curves with the experimental excitation curves. By a series of iterations the parameters describing the ^{18}O concentration profile can be modified to generate theoretical excitation curves that best fit the experimental data. The initial proton beam energy spread (0.8 keV), particle energy straggling, and the finite width of the resonant cross section (2.1 eV) were incorporated into the convolution. The average energy loss for incident protons in the energy range of 600–700 keV is 0.9 keV/nm. A computational program¹¹ was used to generate such curves. For each incident proton energy E_p this program convolutes the energy straggling with the differential cross-section values, providing the probability of creating an α particle at each depth. A matrix of such probabilities is calculated as a function of depth and then again convoluted with the assumed concentration profile in order to produce a calculated excitation curve. The parameter describing this profile, i.e., the oxide thickness, is then adjusted by a subroutine DLMDF1,¹² to fit the experimental data. The convolution program uses experimental cross-section values¹³ interpolated in 0.1-keV steps. For simplicity, step functions were used as profiles since such functions are consistent with the physical nature of growing oxide films. Due to the experimental depth resolution, detailed shape curves could not be resolved for Mg ^{18}O layers less than 20 nm thick. However, the total amount of ^{18}O present near the surface was provided by the analysis, irrespective of the Mg ^{18}O layer thickness. The experimental depth resolution is limited by the width at half maximum amplitude of the $^{18}\text{O}(p,\alpha)^{15}\text{N}$ resonance at 629 keV, by straggling of the protons as they lose energy and by the energy resolu-

tion of the detector. This resolution can be estimated from the uncertainties in values of these various parameters, and in addition it is experimentally determined by the measured width of the peaks with the least amplitude shown in Figs. 3–5. We note that the width at half maximum amplitude of all these peaks is 4 keV. Since these peaks are produced by the Mg ^{18}O layers with thickness less than or equal to 10 nm, and since the width equivalent to 4 keV is about 20 nm, the width equivalent of 4 keV represents the minimum resolvable thickness. The error in measuring thicknesses greater than 20 nm must then be ± 10 nm, which is equivalent to ± 2 keV.

If it is assumed that the detected ^{18}O corresponds to an epitaxial layer of Mg ^{18}O , then one can deduce the layer thickness from the total amount of ^{18}O . The deduced layer thickness permits the following diffusion parameters to be calculated.

A simple charge-mass balance yields the cationic transference number, which is the ratio of the charge moved to the cathode due to cationic drift to the total charge transported through the material:

$$t_{\text{cat}} = \frac{\rho Z F \Delta x}{M J \Delta t} \quad (1)$$

In this expression Z is the charge of the cation, Δt the time interval, F Faraday's constant, ρ the density, M the molecular weight, J the dc current density, and Δx the Mg ^{18}O layer thickness. It is assumed that the surface area of the electrode-sample interface is constant, and that this interface is displaced by Δx normal to the electrode plane. Experimental evidence of such displacement in MgO subjected to electric fields has been shown by coulometric linear expansion.¹⁴

The thickness of the Mg ^{18}O layer also allows the calculation of the ion mobility and diffusion coefficient. By using the relation between conductivity σ and electric field E , $\sigma = J/E$, between the conductivity and mobility μ , $\sigma = Zec\mu$, and the charge-mass balance for pure ionic current flow, $MJ \Delta t = \rho Z F \Delta x$ [Eq. (1) for $t_{\text{cat}} = 1$], an expression for the mobility of the mobile defects can be derived:

$$\mu = \frac{\rho F \Delta x}{ecEM \Delta T} \quad (2)$$

The constant c is the cationic current-carrier concentration.

On the assumption that the mobile defects are doubly charged MgO vacancies, this concentration, $[V_{\text{Mg}}'']$ can be estimated from the charge-balance condition

$$2[V_{\text{Mg}}''] = [I_{\text{Mg}}] \quad (3)$$

where $[I_{\text{Mg}}]$ is the concentration of trivalent solutes; trivalent impurity concentrations measured by neutron activation analysis are used for this estimate. It is assumed

that these impurities are in solid solution. The effect of monovalent ions on the charge compensation is neglected, as has been done in other work;¹⁵ the action of monovalent ions is poorly understood and they may be precipitated. The contribution of silicon is neglected since its solubility is very low.¹⁶

The cation vacancy self-diffusion D is determined from the Nernst-Einstein equation, $D = kT\mu/Ze$, in which the mobility value is replaced by Eq. (2).

To obtain the diffusion coefficient for magnesium ions, the relative concentration of magnesium ions and vacancies, as well as the correlation factor, must be taken into consideration. The correlation factor f compensates for the fact that after a jump of a magnesium ion, the probability of jumping into its previous site (where the vacancy is now residing) is greatly enhanced. Based on geometrical considerations for an fcc lattice, $f = 0.78$.¹⁷ Accordingly,

$$D_{\text{Mg}} = \frac{0.78fkT\rho\Delta x}{MZe^2N_{\text{Mg}}E\Delta t}, \quad (4)$$

where N_{Mg} is the concentration of magnesium ions in MgO ($5.45 \times 10^{22} \text{ cm}^{-3}$). Knowledge of the vacancy concentration is not required to determine the Mg self-diffusion coefficient by this method.

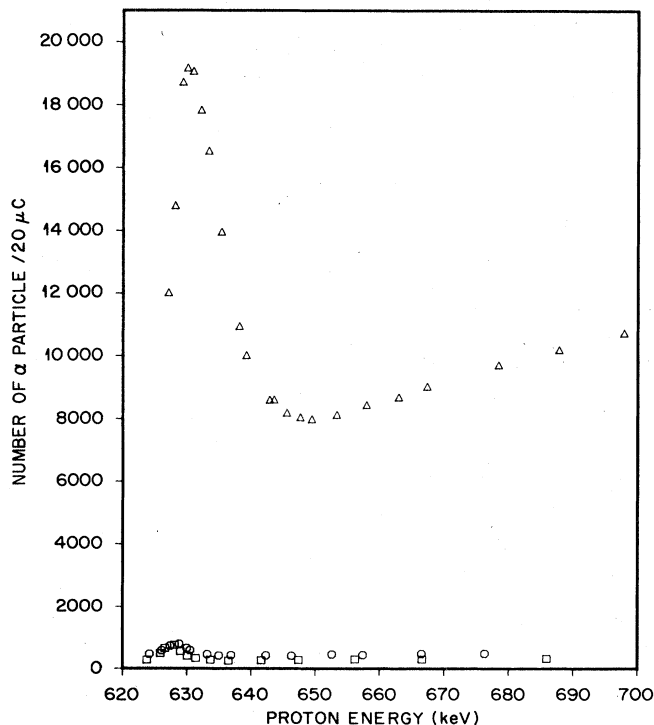


FIG. 2. Excitation curves for an MgO single crystal subjected to isotopic exchange at 930°C for 24 h and to an electric field of 1000 V/cm: Δ cathode side, \circ anode side, and \square no field.

IV. RESULTS

A. Diffusion mechanism for moderate fields

The effect of an electric field on the excitation curves is shown in Fig. 2 for a MgO single crystal subjected to a field of 1000 V/cm during a 24-h $^{18}\text{O}_2$ gas solid exchange at $(930 \pm 2)^\circ\text{C}$. Data from a sample given the same treatment, but without applied field, are included for comparison. The cathode face of the sample annealed in an applied electric field exhibits a much higher particle count than does the anode side. Indeed, this has been observed for all samples subject to moderate electric fields. The anode face exhibits an excitation curve similar to the one obtained without field. Considering the experimental parameters adopted, e.g., temperature, electric field strength, and time interval, the high concentration of ^{18}O in the cathode region cannot be accounted for on the basis of calculations¹¹ using known oxygen diffusivities. A drift mobility for oxygen vacancies more than two orders of magnitude greater than expected from oxygen diffusion¹¹ would be required to fit the observed excitation curve. However, if magnesium vacancies are present in the crystal as charge compensation for aliovalent cationic impuri-

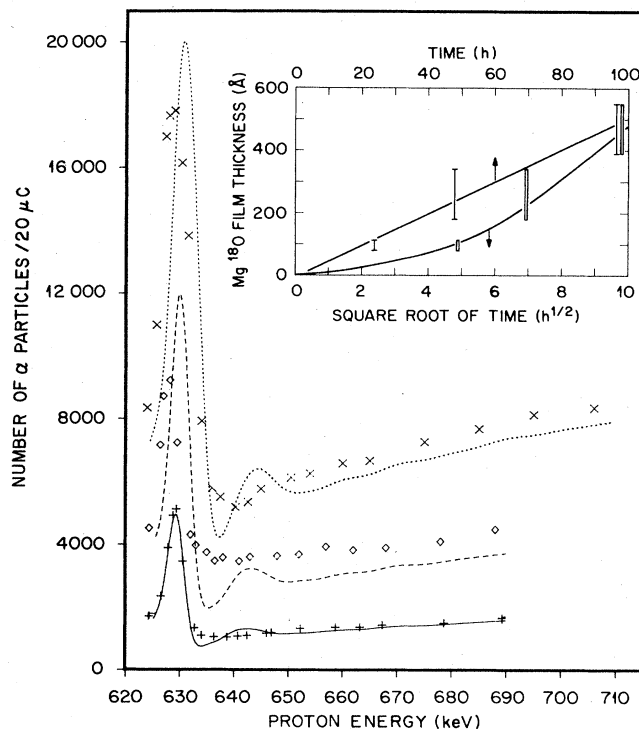


FIG. 3. Excitation curves from the cathode side of MgO single crystals subjected to ^{18}O isotopic exchange at 930°C, and to an electric field of 90 V/cm. Points shown are experimental results for time intervals of 24 h (+), 48 h (\diamond), and 96 h (\times). Lines are calculated excitation curves corresponding to each experimental condition. The inset shows the growth of the Mg^{18}O layer on the surface of the crystal vs time interval and vs the square root of time interval.

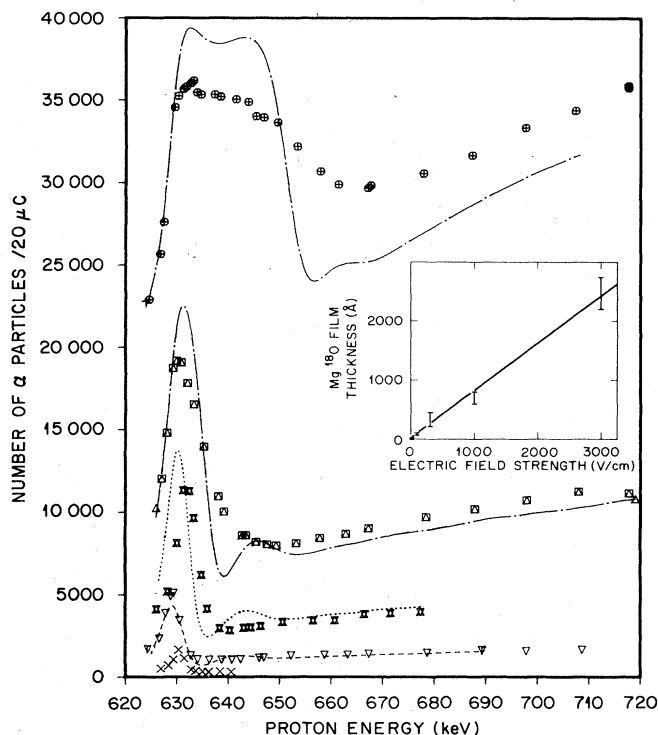


FIG. 4. Excitation curves from the cathode side of MgO single crystals subjected to isotopic exchange at 930°C for 24 h and to electric fields 3000 V/cm (\odot), 1000 V/cm (\square), 300 V/cm (\times), 90 V/cm (∇) and 10 V/cm (\times). Lines are calculated excitation curves corresponding to each experimental condition. The inset shows the Mg¹⁸O layer thickness vs the applied electric field.

ties, the electric field would produce a drift of magnesium ions to the cathode, where the excess Mg would react with ¹⁸O₂ and form an Mg¹⁸O layer.

In order to identify the process which causes a higher concentration of ¹⁸O at the cathode in comparison to that at the anode, we measured the time and field-strength dependence of the total amount of ¹⁸O at the cathode. If the ¹⁸O were diffusing from the surface, then the total amount present would increase as $\sqrt{E \Delta t}$, where E is the electric field and Δt is the anneal time. On the other hand, for magnesium drift through the sample and epitaxial growth of Mg¹⁸O at the cathode, the total amount of oxygen in the layer would increase as $E \Delta t$. Figures 3 and 4 are excitation curves for samples treated at 930°C for different times and with different electric field strengths.

$$D_{\text{Mg}} = (8.84 \pm 1.44) \times 10^{-6} \exp[(-215 \pm 18 \text{ kJ/mol} = 2.23 \pm 0.19 \text{ eV/atom})/kT] \text{ (cm}^2/\text{s)}. \quad (5)$$

If impurities such as Al, Cr, and Fe are considered to be in the trivalent state, their concentration, i.e., 65 mol ppm Al, 6 mol ppm Cr, and 51 mol ppm Fe, can be used in Eq. (3) to estimate the vacancy concentration of $2.97 \times 10^{18} \text{ cm}^{-3}$. Then the diffusion coefficient for cation vacancies can be obtained from the expression

TABLE II. Cationic transference numbers in MgO.

T (K)	t_{cat}	Reference
1507	0.31	Gauthier <i>et al.</i>
1428	0.44	Gauthier <i>et al.</i>
1243	0.37 ± 0.12	Present work
1206	0.48 ± 0.11	Present work
1168	0.45 ± 0.11	Present work
1203	0.80 ± 0.15	MgO:Cr, present work

The data point symbols are experimental results; the curves are best-fit calculated excitation curves, where the total amount of ¹⁸O has been allowed to vary. The inset in Fig. 3 in which the Mg¹⁸O film thickness Δx is plotted versus $\sqrt{\Delta t}$ and versus Δt shows clearly that the Δx versus Δt fit produces a straight line, whereas the square-root fit does not. Similarly, the inset in Fig. 4 shows a linear relation between the Mg¹⁸O— layer thickness calculated from these excitation curves and the field strength.

B. Transference numbers

The cationic transference number can be determined from Eq. (1). The average value of dc current measured during a diffusion anneal is used in this equation. Table II shows the transference numbers determined. These values fall in the same range as those reported for MgO equilibrated at 1428 and 1507 in 1 atm of oxygen.¹⁴ Notice that there is an apparent trend of increased cationic transference numbers at lower temperatures.

C. The temperature dependence

The temperature dependence of the excitation curves was determined for the cathode side by keeping the electric field strength (90 V/cm) constant and varying the temperature. The isotopic exchange time intervals were fixed at 48 h for $T \geq 890^\circ\text{C}$, and 139 h for $T < 890^\circ\text{C}$. Figure 5 shows the results (point symbols) along with the best-fit excitation curves. Clearly the areas under these curves, which are proportional to the ¹⁸O concentration, increase with temperature. Using Eq. (4), diffusion coefficients for magnesium ions were calculated from the oxide thicknesses. These diffusion coefficients have been plotted versus reciprocal temperature in Fig. 6, together with diffusion coefficients obtained by other investigators. Our results, neglecting the lowest temperature point, which will be discussed later, yield the following temperature dependence:

$$D_{V_{\text{Mg}}}'' / D_{\text{Mg}} = 1/fN_v, \text{ where } N_v \text{ is the fraction of vacant Mg sites. Then}$$

$$D_{V_{\text{Mg}}}'' = (0.3 \pm 0.3) \exp[-(215 \pm 18 \text{ kJ/mol})/kT] \text{ (cm}^2/\text{s)}. \quad (6)$$

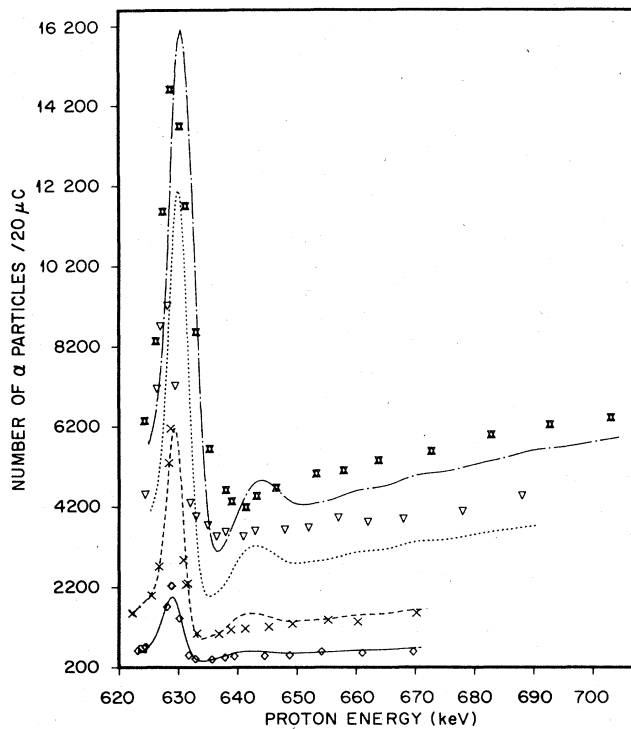


FIG. 5. Excitation curves from the cathode side of MgO single crystals subjected to an electric field strength of 90 V/cm, and ^{18}O isotopic exchange for 48 h at 973°C (XX), 936°C (V), 894°C (X), and for 139.1 h at 845°C (D). Lines are calculated excitation curves corresponding to the experimental conditions.

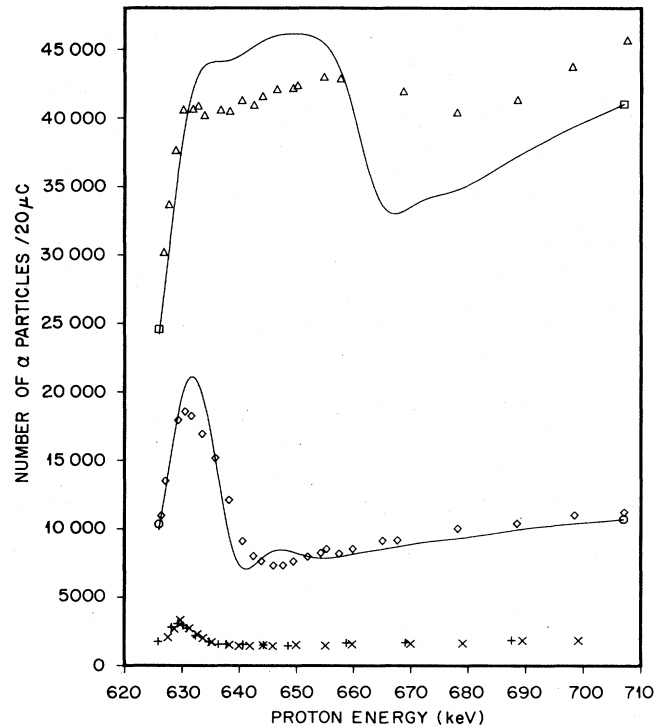


FIG. 7. Excitation curves for Cr-doped MgO and a nominally pure MgO single crystal subjected to 1000 V/cm in an atmosphere of $^{18}\text{O}_2$ for 24 h at 930°C. Experimental data are for cathode side of Cr-doped MgO (Δ), cathode side of nominally pure MgO (\diamond), anode side of Cr-doped MgO (\times), and anode side of nominally pure MgO ($+$). Lines shown for the cathode sides are calculated curves.

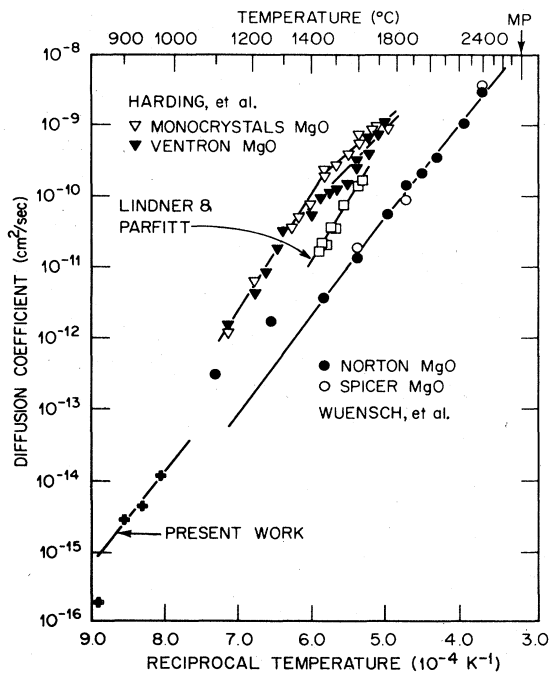


FIG. 6. Comparison of Mg diffusion data of the present work with that of Harding *et al.* (Ref. 22), Lindner and Parfitt (Ref. 23), and Wuensch *et al.* (Ref. 18). MP is the melting point.

D. Effect of added trivalent impurity

The experimental curves obtained from both the cathode and anode faces of a magnesium oxide sample containing 1154 mol ppm chromium and a nominally pure MgO crystal are shown in Fig. 7. It is clear from these data that the thickness of the Mg^{18}O layer at the cathode of the Cr-doped MgO is greater than that of the nominally pure MgO. The anode regions exhibit the same amount of ^{18}O , in agreement with the results described above. Solid lines are fitted excitation curves for the cathode sides; the Mg^{18}O layer thicknesses for these fits are 354 ± 35 nm for the Cr-doped MgO and 82 ± 10 nm for the nominally pure MgO.

V. DISCUSSION

With the technique employed here, it has been possible to measure the self-diffusion coefficients at much lower temperatures than have previously been used and at treatment times that are of short (~ 100 h) duration. The magnesium coefficients obtained are in good agreement with those expected by extrapolating the higher temperature values reported by Wuensch.¹⁸ No significant change in activation energy is observed in this range of temperature, except for the lowest experimental point. This point may indicate that at temperatures $\leq 845^\circ\text{C}$ the activation

energy changes. However, further experimental evidence is needed to support this suggestion. It is reasonable to consider that the temperature range of the present experiment is an extension of the extrinsic region for diffusion. In this region, diffusion is controlled by chemically created vacancies with energies of motion of the order of 2 eV. The preexponential factor and the activation energy for V''_{Mg} diffusion calculated here are in good agreement with the values reported by Sempolinski¹⁹ from ionic conductivity measurement in MgO.

A comparison of the calculated excitation curves with the experimental data shows a relatively poor fit when large oxide layers are present, as is the case when 3000 V/cm is applied. The reason for this poor fit may be due to alterations of the surface texture arising from inhomogeneous electric fields and consequent variations in the growth of the oxide layer. Such alterations have been observed by scanning electron microscopy (SEM).¹¹ At fields lower than 300 V/cm, these features were not observed. SEM micrographs¹¹ from thick Mg¹⁸O layers showed deviations from surface flatness.

The results obtained from the Cr-doped MgO support the assumption that V''_{Mg} are present due to trivalent impurities. EPR measurements²⁰ have shown that chromium normally is in the 3+ valence state in untreated MgO and that reduction or oxidation by ambient gas has no major influence on the Cr³⁺ concentration. A comparison of the Cr concentration obtained from Eq. (3) and that measured by neutron activation shows that approximately 30% of the total chromium takes part in the transport process. This result is in agreement with the decrease of Cr³⁺ concentration detected by ERP on crystals subjected to field of 1000 V/cm at 1100°C.²¹ The disappearance or large decrease of EPR lines due to Cr³⁺ indicates that Cr³⁺ is changing its charge state, probably to Cr²⁺. Also, Cr ions may be present as pairs or triplets, which decreases their participation in the ionic transport process.

The cationic transference number, calculated from Eq.

(1) for Cr-doped MgO, is $t_{cat} = 0.80 \pm 0.15$. This value is higher than that calculated for nominally pure MgO ($t_{cat} = 0.54 \pm 0.10$), which suggests that the additional chromium increases the transport of Mg ions by increasing the extrinsic vacancy concentration. It is noted that Sempolinski *et al.*²⁴ have shown that the cationic transference number of nominally pure MgO crystals with compositions similar to those used in these experiments is ~ 0.5 . Thus the electronic contribution to the conductivity is a major fraction of the measured conductivity.

VI. CONCLUSIONS

The measurement of ¹⁸O concentration in the cathode region of MgO crystals subjected to moderate electric fields provides a method for the determination of magnesium diffusion coefficients, cationic transference numbers, and, within the accuracy of determining the cation vacancy concentration, vacancy diffusion coefficients. The present results are explained by the migration of vacancies toward the anode. The diffusivity of Mg ions is shown to follow an Arrhenius function observed at high T (1800–2000 K) down to $T \geq 1100$ K. Cationic transference numbers for nominally pure MgO crystals have values in the range 0.37–0.50; those for Cr-doped MgO crystals are approximately 0.8. Results on Cr-doped crystals support the assumption that V''_{Mg} are present due to trivalent impurities.

ACKNOWLEDGMENTS

This research was supported by the Division of Materials Sciences, U. S. Department of Energy under Contract No. DE-AC05-84OR21400 with Martin Marietta Energy Systems, Inc. This is a portion of the research submitted by J. R. Martinelli to Vanderbilt University in partial fulfillment of the requirements for the Ph.D. degree.

¹E. Sonder, K. F. Kelton, J. C. Pigg, and R. A. Weeks, *J. Appl. Phys.* **49**, 5971 (1978).

²R. A. Weeks, J. Narayan, and E. Sonder, *Phys. Status Solidi A* **70**, 639 (1981).

³V. C. Nelson and R. J. Friauf, *J. Phys. Chem. Solids* **31**, 825 (1970).

⁴Ya. E. Geguzin, V. I. Solunskii, and Yu. I. Boiko, *Fiz. Tverd. Tela (Leningrad)* **8**, 1304 (1966) [*Sov. Phys.—Solid State* **8**, 1046 (1966)].

⁵K. J. D. MacKenzi, R. K. Banerjee, and M. R. Kasaai, *J. Mater. Sci.* **14**, 333 (1979).

⁶K. J. D. MacKenzie and R. K. Banerjee, *J. Mater. Sci.* **14**, 339 (1979).

⁷K. J. D. MacKenzie and M. J. Ryan, *J. Mater. Sci.* **16**, 579 (1981).

⁸P. Kofstad, *Nonstoichiometry, Diffusion, and Electrical Conductivity of Binary Metal Oxides* (Wiley-Interscience, New York, 1972), p. 121.

⁹Tateho Chemical Industries Co., Ltd., Hyogo-Ken, Japan.

¹⁰E. Sonder, J. V. Spadaro, and R. A. Weeks, *J. Am. Ceram. Soc.* **64**, C-65 (1981).

¹¹J. R. Martinelli, Ph.D. dissertation, Vanderbilt University, 1984.

¹²B. S. Garbow, K. E. Hillstrom, and J. M. More, Minpack Documentation, Argonne National Laboratory, Argonne, IL, 1980 (unpublished). The fitting method is described in this reference.

¹³*Ion Beam Handbook for Materials Analysis*, edited by J. W. Mayer and E. Rimini (Academic, New York, 1977).

¹⁴M. Gauthier, P. Fabry, and C. Deportes, *Electrochem. Acta* **19**, 103 (1974).

¹⁵B. J. Wuensch, *Mater. Sci. Res.* **9**, 211 (1975).

¹⁶A. F. Henriksen, Sc.D. thesis, Massachusetts Institute of Technology, Cambridge, Massachusetts, 1978.

¹⁷P. Kofstad, *Nonstoichiometry, Diffusion, and Electrical Conductivity of Binary Metal Oxides* (Wiley-Interscience, New York, 1972), p. 81.

¹⁸B. J. Wuensch, W. C. Steele, and T. Vasilos, *J. Chem. Phys.* **58**, 5258 (1973).

¹⁹D. R. Sempolinski and W. D. Kingery, *J. Am. Ceram. Soc.*

- 63, 664 (1980).
- ²⁰R. A. Weeks and E. Sonder, *Rev. Int. Hautes Temp. Refract.* **17**, 154 (1980).
- ²¹R. A. Weeks, E. Sonder, J. C. Pigg, and K. F. Kelton, *J. Phys. Suppl.* **37**, 411 (1976).
- ²²B. C. Harding, D. M. Price, and A. J. Mortlock, *Philos. Mag.* **23**, 399 (1971).
- ²³R. Lindner and G. D. Parfitt, *J. Chem. Phys.* **26**, 182 (1957).
- ²⁴D. R. Sempolinskii, W. D. Kingery, and H. L. Tuller, *J. Am. Ceram. Soc.* **63**, 669 (1983).